



Cite this: *Catal. Sci. Technol.*, 2025, 15, 5066

## A quantitative analysis of the impact of SO<sub>2</sub> on the activity of Cu-CHA catalysts for NH<sub>3</sub>-SCR†

Reza K. Abasabadi, <sup>ab</sup> Ton V. W. Janssens <sup>a</sup> and Gloria Berlier <sup>\*b</sup>

Copper-exchanged chabazite (Cu-CHA) catalysts for selective catalytic reduction of NO<sub>x</sub> by ammonia (NH<sub>3</sub>-SCR) in diesel exhausts deactivate in the presence of SO<sub>2</sub> at temperatures below 300 °C. In this article, we develop a descriptive model to evaluate a catalyst deactivation with respect to SO<sub>2</sub> tolerance, in terms of a disappearance of active catalyst. This leads to the SO<sub>2</sub> sensitivity, which can be interpreted as the loss of catalyst per mol SO<sub>2</sub> taken up by the catalyst, as a measure for the deactivation for that catalyst material. We have determined the SO<sub>2</sub> sensitivity for three Cu-CHA catalysts, namely 1.6 and 3.2 wt% Cu with a Si/Al ratio of 6.7 and 3.2 wt% Cu with a Si/Al ratio of 15. The 3.2 wt% Cu (Si/Al = 6.7) catalyst shows a lower SO<sub>2</sub> sensitivity at 200 °C, as compared to the other two catalysts. For all three catalysts, the SO<sub>2</sub> sensitivity is highest at low SO<sub>2</sub> uptake, and decreases linearly with the further uptake of SO<sub>2</sub>. This means that small amounts of SO<sub>2</sub> cause a relatively strong deactivation, indicating that the deactivation is a consequence of a reaction of SO<sub>2</sub> with the active Cu.

Received 17th February 2025,  
Accepted 15th July 2025

DOI: 10.1039/d5cy00188a

rsc.li/catalysis

## 1 Introduction

Cu-exchanged chabazite (Cu-CHA) zeolites are the state-of-the-art catalysts for the selective catalytic reduction of nitrogen oxides (NO<sub>x</sub>) by ammonia in presence of oxygen (O<sub>2</sub>) for mobile applications.<sup>1–3</sup> This reaction, in which the NO<sub>x</sub> reacts with ammonia to N<sub>2</sub> and H<sub>2</sub>O, forms the basis of the current NO<sub>x</sub> emission control technologies applied in diesel vehicles.<sup>4,5</sup> Cu-CHA materials have a good activity in the range 150–550 °C, and can tolerate exposures to temperatures over 700 °C,<sup>6–8</sup> which means that these materials are compatible with the harsh and dynamic conditions in an exhaust pipe.

The activity of Cu-CHA catalysts for NH<sub>3</sub>-SCR, however, is sensitive to the presence of SO<sub>2</sub>, in particular at temperatures below 300 °C.<sup>9–13</sup> Therefore, the application of Cu-CHA catalysts is recommended only in combination with ultra-low sulfur diesel fuel, and a proper operation of the catalyst to minimize the impact of SO<sub>2</sub>.<sup>14,15</sup>

A first explanation for the deactivation by SO<sub>2</sub> is that the formation of ammonium sulfate or ammonium bisulfate under the conditions for NH<sub>3</sub>-SCR makes the active centers inaccessible for the NO and NH<sub>3</sub> reactants.<sup>16–20</sup> An effective physical blocking of the active centers by deposition of

ammonium sulfate or ammonium bisulfate requires larger amounts of ammonium sulfates to be deposited in the catalysts. However, the catalytic activity of a Cu-CHA catalyst around 200 °C is reduced by about 80% at S/Cu ratios of 0.2–0.3,<sup>11,12,21</sup> indicating that deactivation is almost complete at a molar amount of SO<sub>2</sub> that is 4–5 times lower than the active Cu content. Furthermore, V<sub>2</sub>O<sub>5</sub>/TiO<sub>2</sub> and Fe-zeolite based catalysts for NH<sub>3</sub>-SCR show a significantly better tolerance for SO<sub>2</sub> under similar process conditions, in particular below 300 °C,<sup>22–24</sup> indicating that the formation of ammonium sulfate or ammonium bisulfate requires some influence of the catalyst. These observations seem inconsistent with a mechanism relying on deposition of ammonium sulfate, and indicate that the SO<sub>2</sub>-induced deactivation of Cu-CHA catalysts is a consequence of a direct interaction of SO<sub>2</sub> with the active Cu-centers.<sup>25,26</sup>

Recently, it has been shown, that SO<sub>2</sub> preferably interacts with  $[(\text{NH}_3)_4\text{Cu}_2^{\text{II}}\text{O}_2]^{2+}$  complexes ( $\mu\text{-}\eta^2,\eta^2\text{-peroxo diamino dicopper(II)}$ ) in Cu-CHA catalysts, while Cu<sup>I</sup> species show virtually no interaction with SO<sub>2</sub>.<sup>27–29</sup> Below 300 °C, these  $[(\text{NH}_3)_4\text{Cu}_2^{\text{II}}\text{O}_2]^{2+}$  complexes are formed upon oxidation of mobile  $[(\text{NH}_3)_2\text{Cu}^{\text{I}}]^+$  species by oxygen.<sup>30–34</sup> The NH<sub>3</sub>-SCR reaction proceeds *via* a reaction of NO with these  $[(\text{NH}_3)_4\text{Cu}_2^{\text{II}}\text{O}_2]^{2+}$  complexes, and the reaction of SO<sub>2</sub> reduces the rate of this reaction with NO,<sup>35</sup> leading to the deactivation of the catalyst for NH<sub>3</sub>-SCR. Because in this scenario, the catalyst deactivation involves the  $[(\text{NH}_3)_4\text{Cu}_2^{\text{II}}\text{O}_2]^{2+}$  complexes, the deactivation is enhanced under process conditions that favor the formation of the  $[(\text{NH}_3)_4\text{Cu}_2^{\text{II}}\text{O}_2]^{2+}$  complexes. This is supported by the observation that the uptake of sulfur upon exposing a Cu-CHA catalyst to SO<sub>2</sub> is significantly reduced, after

<sup>a</sup> Umicore Denmark ApS, Kogle Allé 1, 2970 Hørsholm, Denmark

<sup>b</sup> Department of Chemistry and NIS Centre, University of Turin, Via Giuria 7, 10125 Turin, Italy. E-mail: gloria.berlier@unito.it

† Electronic supplementary information (ESI) available. See DOI: <https://doi.org/10.1039/d5cy00188a>



reduction of the Cu to a Cu<sup>I</sup> state, while it is enhanced in the presence of oxygen.<sup>28,29</sup> The insight that the impact of SO<sub>2</sub> depends on the actual state of the Cu in the catalyst implies that the deactivation behavior of a catalyst does not only depend on the material properties of the catalyst, but also on the conditions the catalyst is exposed to.<sup>36,37</sup> Therefore, a model describing the deactivation behavior of Cu-CHA catalysts must also contain a record for the process conditions the catalyst has been exposed to.

In this article, we construct a descriptive model for the deactivation of Cu-CHA catalysts by SO<sub>2</sub>. In the model, the deactivation is described in terms of a decrease of the amount of active catalyst. This concept has been applied earlier to characterize the deactivation of zeolite catalysts used for the methanol-to-hydrocarbons reaction.<sup>38,39</sup> Foley *et al.* have categorized the deactivation behavior of catalysts in non-selective and selective deactivation.<sup>38</sup> Non-selective deactivation means that the catalyst becomes less active, without any further changes in the catalytic behavior. Deactivation by loss of active sites falls in this category. Therefore, for non-selective deactivation, it is possible to describe the activity at any point of the deactivation process in terms of a corresponding amount of fresh catalyst, effectively leading to a variable amount of catalyst as the deactivation progresses. With selective deactivation, the catalytic reaction or catalyst itself changes, such that the performance of the catalyst can no longer be described adequately as a loss of catalyst amount.<sup>38</sup> To model the deactivation of SO<sub>2</sub>, we assume that the SO<sub>2</sub> only leads to a loss of active Cu, without further changes to the NH<sub>3</sub>-SCR reaction cycle, and have therefore used the non-selective approach.

A natural descriptor for the deactivation process would be the time, in analogy to the description of the deactivation of zeolites in the methanol-to-hydrocarbon reaction,<sup>38,39</sup> which then leads to a time-dependent amount of catalyst in the model. However, this leads to ambiguous results for the deactivation of Cu-CHA catalysts by SO<sub>2</sub>. A better description of the deactivation is obtained by using the accumulated amount of SO<sub>2</sub> in the catalyst ( $n_{SO_2}$ ), and the deactivation model is adapted by directly replacing the time parameter with the accumulated amount of SO<sub>2</sub>. Consequently, the deactivation model requires measurement of the conversion at different amounts of SO<sub>2</sub> for different ratios of the amount of catalyst and flow (W/F ratio in g<sub>cat</sub> h mol<sup>-1</sup>). With this approach we obtain a quantification of the deactivation by SO<sub>2</sub>, without making explicit assumptions on the deactivation behavior. A combination of such a description of deactivation with reaction kinetics is then capable of describing the behavior of a Cu-CHA catalyst upon exposure to SO<sub>2</sub>, thus providing a tool to characterize Cu-CHA materials with respect to their deactivation behavior in the presence of SO<sub>2</sub>.

In this study, we evaluate the deactivation from measurements of the NO<sub>x</sub> conversion at 200 °C for different W/F ratios and different amounts of SO<sub>2</sub> in the catalyst, with the aim understand the deactivation by SO<sub>2</sub> based on the

chemistry and material properties of the catalyst. To reduce the complexity of the system, we exclude a possible effect of H<sub>2</sub>O on the deactivation by SO<sub>2</sub>, since the effect of water on the interaction of SO<sub>2</sub> with the  $[(NH_3)_4Cu_2^{II}O_2]^{2+}$  complex is still not known. By applying the method to three Cu-CHA based catalysts with different Cu loading and Si/Al ratios, we obtain insight into the deactivation behavior of these catalysts, based on the uptake of SO<sub>2</sub> by these catalysts.

## 2 Measurement of deactivation

### 2.1 Method

An essential characteristic of catalyst deactivation is the change of the activity of a catalyst with *time*, possibly accompanied with a change in other properties, such as selectivity or reaction products. Applying this concept to the deactivation of Cu-CHA catalysts by SO<sub>2</sub>, the deactivation is then described by the time of exposure to SO<sub>2</sub>, at a well defined temperature and partial pressure of SO<sub>2</sub>. In the following, we derive an expression for the deactivation in terms of SO<sub>2</sub> exposure time, and show how this leads to ambiguous results. The ambiguity is then removed by exchanging the time variable with the accumulated amount of SO<sub>2</sub> in the catalyst.

In a deactivation measurement, the catalyst deactivation is observed as a change in the conversion during exposure to SO<sub>2</sub>, while keeping the flow, the partial pressure of SO<sub>2</sub>, and temperature constant. Following the concept as applied earlier for the methanol-to-hydrocarbon reaction over zeolite catalysts,<sup>38,39</sup> the change in conversion with exposure time to SO<sub>2</sub> is described by applying the chain rule for differentiation as follows:

$$\frac{dX}{dt_{SO_2}} = \frac{dX}{d\tau} \cdot \frac{d\tau}{dt_{SO_2}} = \frac{dX}{d\tau} \cdot \frac{1}{F} \frac{dW(t)}{dt_{SO_2}} \quad (1)$$

For a plug flow reactor, the derivative dX/dτ is the reaction rate, and thus eqn (1) describes the deactivation by multiplication of the rate with a time-dependent factor dτ/dt<sub>SO<sub>2</sub></sub>. In this article, we express the activity, or rate constant, in terms of the amount of catalyst, and therefore τ refers to a “contact time” expressed as the ratio of the amount of catalyst and flow (W/F). Introducing this definition of τ in the equation, the time-dependent term reflects a rate of change in catalyst amount as a description of the deactivation.

To determine the term dτ/dt<sub>SO<sub>2</sub></sub> from experimental data, eqn (1) is rewritten as:

$$\frac{d\tau}{dt_{SO_2}} = \left[ \frac{\frac{dX}{dt_{SO_2}}}{\frac{dX}{d\tau}} \right] \quad (2)$$

The right hand side of eqn (2) contains the terms dX/dt<sub>SO<sub>2</sub></sub> and dX/dτ, which both can be determined experimentally. The deactivation is then quantified as the ratio of the measured changes in conversion as a function of the exposure time to SO<sub>2</sub> and the measured rate of the fresh

catalyst. In this way, a value for the term  $d\tau/dt_{SO_2}$  can be determined based on experimentally accessible data.

Because the interaction of  $SO_2$  with a Cu-CHA catalyst depends on the state of the Cu in the catalyst, the impact of  $SO_2$  exposure does not remain constant on the time scale of our measurement. Therefore, the exposure time is not a good descriptor for the deactivation process. It has been shown that the  $SO_2$  uptake takes place through a reaction of  $SO_2$  with the  $[(NH_3)_4Cu_2^{II}O_2]^{2+}$  complex, under the formation of some  $Cu^{I}$  species that does not react with  $SO_2$ .<sup>27-29</sup> Consequently, if the Cu-CHA is prepared such that all Cu is present as the  $[(NH_3)_4Cu_2^{II}O_2]^{2+}$  complex, exposure of the catalyst to  $SO_2$  does not result in a complete saturation of the catalyst, or deactivation of the catalyst. A reoxidation and subsequent exposure to  $SO_2$  will result in additional uptake of  $SO_2$  and deactivation.<sup>28</sup> Therefore, by repeating cycles of reduction, oxidation, and  $SO_2$  exposure, a stepwise  $SO_2$  uptake and deactivation occurs. This is further illustrated in Fig. 1a, which shows the measured NOx conversion and cumulative uptake of  $SO_2$  in six consecutive cycles.

This stepwise uptake of  $SO_2$ , and the accompanying changes in the state of the Cu in the catalyst, leads to an inadequate description of the deactivation process in terms of  $SO_2$  exposure time. This can be understood as follows. An arbitrary extension of the  $SO_2$  exposure time in each cycle as shown in Fig. 1b from 45 min by, for example, 1 hour, or shortening it to 30 min., does not significantly affect the  $SO_2$  uptake and measured NOx conversion, as the catalyst saturates after about 30 min in each cycle. However, such changes in exposure time  $t_{SO_2}$  in each step leads to different total exposure times. Consequently, an evaluation of  $d\tau/dt_{SO_2}$  according to eqn (2) results in a different values that depends on an arbitrarily chosen exposure time ( $t_{SO_2}$ ) in each cycle, resulting in ambiguous results for the value of  $d\tau/dt_{SO_2}$ .

Since the data in Fig. 1a indicate that the decrease in conversion follows the  $SO_2$  uptake, the accumulated amount

of  $SO_2$  in the catalyst ( $n_{SO_2}$ ) seems to be a more appropriate descriptor for the deactivation process. To implement this change of descriptor in the model, eqn (2) is adapted by replacing  $t_{SO_2}$  with  $n_{SO_2}$ , resulting in:

$$\frac{d\tau}{dn_{SO_2}} = \frac{\left[ \frac{dX}{dn_{SO_2}} \right]}{\left[ \frac{dX}{d\tau} \right]} \quad (3)$$

In eqn (3), the deactivation is then quantified by the term  $d\tau/dn_{SO_2}$ . This term represents a change in effective catalyst amount as a consequence of some uptake of  $SO_2$ ; the unit of  $d\tau/dn_{SO_2}$  becomes  $g_{cat}^{-2} h mol^{-2}$ . A high value for  $d\tau/dn_{SO_2}$  means that a large amount of catalyst is affected by a smaller amount of  $SO_2$ , and therefore, this value can be interpreted as a sensitivity of a catalyst for  $SO_2$ . In this article, we use this as the parameter describing the catalyst deactivation. The term  $dX/d\tau$  refers to the rates measured for a fresh catalyst.

## 2.2 Experimental

The Cu ion-exchanged chabazite (Cu-CHA) catalysts used in this study contain 3.2 wt% and 1.6 wt% Cu with a Si/Al ratio of 6.7, and 3.2 wt% Cu with a Si/Al ratio of 15. The Cu-CHA catalysts were prepared by impregnation of the parent chabazite material (Si/Al = 6.7 or 15), through spraying with an amount of an aqueous solution of Cu-nitrate that matches the desired Cu content. The mixture was dried at 90 °C until all the liquid evaporated, followed by calcination in air at 600 °C for 2 h to decompose the nitrates.

To measure the deactivation in terms of the sensitivity for  $SO_2$ , the conversion of NOx is determined for different values of  $\tau$ , and  $n_{SO_2}$ . The measurements of the NOx conversion were conducted in a quartz U-tube powder reactor with a 4 mm inner diameter, using 5 or 10 mg catalyst (sieve fraction 150–300  $\mu m$ ). The reactor was connected to an FTIR spectrometer for gas composition analysis at the reactor

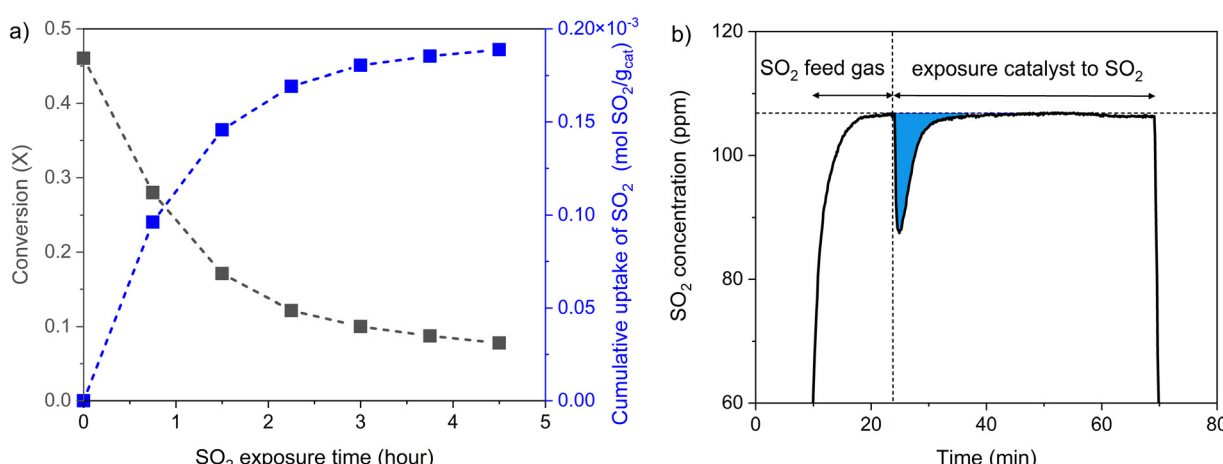


Fig. 1 a) Measured conversion and accumulated  $SO_2$  uptake in six consecutive  $SO_2$  exposure cycles at 200 °C after formation of the  $[(NH_3)_4Cu_2^{II}O_2]^{2+}$  complex. b) Measured  $SO_2$  concentration during exposure to  $SO_2$ . The blue area represents the uptake of  $SO_2$ . Catalyst 3.2 wt% Cu-CHA, Si/Al ratio 6.7.



outlet. Initially, the catalysts were heated to 550 °C in an atmosphere containing 10% O<sub>2</sub>. The reactor was cooled to 200 °C to carry out the remaining procedure at this temperature. Subsequently, the activity of catalysts was measured using a gas mixture containing 500 ppm NO, 600 ppm NH<sub>3</sub>, 5% H<sub>2</sub>O and 10% O<sub>2</sub> at a total flow of 10, 11.1, 12.5, 14.3, 16.7 and 20 Nl h<sup>-1</sup>. The flow values correspond to contact times  $\tau$  = 0.0054, 0.0065, 0.0076, 0.0087, 0.0098 and 0.0108 g<sub>cat</sub> h mol<sup>-1</sup> for a 5 mg sample and  $\tau$  = 0.0112, 0.0134, 0.0157, 0.0179, 0.0201 and 0.0224 g<sub>cat</sub> h mol<sup>-1</sup> for a 10 mg sample. The values for dX/dτ were determined based on these measurements. After the activity measurements, the catalysts were prepared in different ways before the exposure to SO<sub>2</sub>, in order to measure the dX/dn<sub>SO<sub>2</sub></sub>. The different preparations were:

1. Reduction in NO/NH<sub>3</sub> followed by oxidation in 10% O<sub>2</sub>, which results in the formation of the  $[(\text{NH}_3)_4\text{Cu}_2^{\text{II}}\text{O}_2]^{2+}$  complex.<sup>27</sup>
2. Reduction in NO/NH<sub>3</sub>, resulting in the formation of  $[(\text{NH}_3)_2\text{Cu}^{\text{I}}]^{+}$ .<sup>27,33</sup>
3. exposure to a dry NH<sub>3</sub>-SCR feed gas (500 ppm NO/600 ppm NH<sub>3</sub>/10% O<sub>2</sub>).

Further details for these procedures are provided in the Supporting Information. After these preparations, the catalysts were exposed to 100 ppm SO<sub>2</sub>/N<sub>2</sub> at 200 °C for 45 min, followed by an activity measurement at different flows, and in the case of the  $[(\text{NH}_3)_4\text{Cu}_2^{\text{II}}\text{O}_2]^{2+}$  complex, prepared according to 1 in the list above, also to 100 ppm SO<sub>2</sub> in the presence of a 800 ppm NO/960 ppm NH<sub>3</sub> mixture, or 10% O<sub>2</sub>. The entire measurement consists of six consecutive cycles consisting of a preparation step, a SO<sub>2</sub> exposure step and a measurement of the catalytic activity. The uptake of SO<sub>2</sub> in each sulfation step was determined by integration of the measured SO<sub>2</sub> concentration (see Fig. 1b, and the total amount of SO<sub>2</sub> is determined by addition of the SO<sub>2</sub> uptake in each individual SO<sub>2</sub> exposure step. From these measurements, the values for dX/dn<sub>SO<sub>2</sub></sub> were determined (Fig. S6–S9 in ESI<sup>†</sup>).

### 3 Results

Fig. 2 shows the uptake of SO<sub>2</sub> under different conditions for the SO<sub>2</sub> exposure and different preparations of the catalyst (3.2 wt% Cu-CHA Si/Al = 6.7) over six consecutive cycles. Exposure of the catalyst to SO<sub>2</sub> after reduction (Cu<sup>I</sup> species, brown) results in a very low uptake of SO<sub>2</sub>, in agreement with earlier observations that SO<sub>2</sub> does not react with Cu<sup>I</sup>.<sup>27,29</sup> The formation of  $[(\text{NH}_3)_4\text{Cu}_2^{\text{II}}\text{O}_2]^{2+}$  complex followed SO<sub>2</sub> exposure results in a higher SO<sub>2</sub> uptake which reaches a stable level after 4/5 cycles (blue). The uptake is faster (reaching a plateau already after 2 cycles) and higher when the  $[(\text{NH}_3)_4\text{Cu}_2^{\text{II}}\text{O}_2]^{2+}$  complex is exposed to SO<sub>2</sub> and O<sub>2</sub> (green). This has been explained by the reoxidation of the Cu<sup>I</sup> formed in the reaction with SO<sub>2</sub>, to make more  $[(\text{NH}_3)_4\text{Cu}_2^{\text{II}}\text{O}_2]^{2+}$  complexes available for additional reactions with SO<sub>2</sub>.<sup>28</sup> When an NO/NH<sub>3</sub> mixture is present with SO<sub>2</sub>

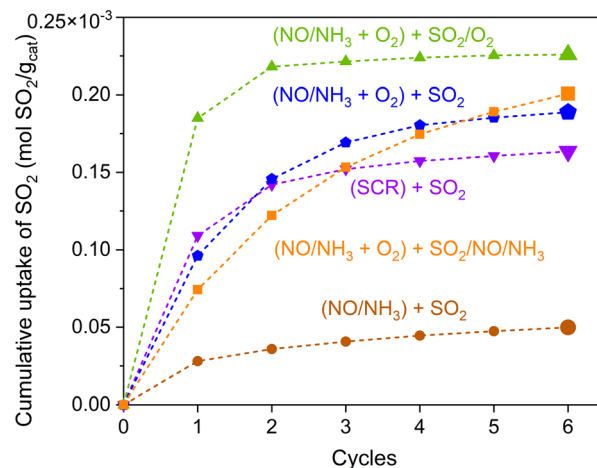


Fig. 2 Measured SO<sub>2</sub> uptakes for a Cu-CHA catalyst with Cu loading 3.2 wt% and Si/Al ratio of 6.7 at 200 °C, under the conditions of SO<sub>2</sub> exposure to reduced Cu<sup>I</sup> (brown), SO<sub>2</sub> exposure to the  $[(\text{NH}_3)_4\text{Cu}_2^{\text{II}}\text{O}_2]^{2+}$  complex (blue), SO<sub>2</sub> in presence of O<sub>2</sub> (green) or NO/NH<sub>3</sub> mixture (orange) to the  $[(\text{NH}_3)_4\text{Cu}_2^{\text{II}}\text{O}_2]^{2+}$  complex, and SO<sub>2</sub> exposure after exposure to dry SCR reaction gas mixture (purple). SO<sub>2</sub> concentration: 100 ppm.

during the reaction with the  $[(\text{NH}_3)_4\text{Cu}_2^{\text{II}}\text{O}_2]^{2+}$  complex (orange), the uptake of SO<sub>2</sub> is at first lower than the previous case, but steadily increases and does not reach a plateau after 6 cycles, at variance with the other conditions. After conditioning of the Cu-CHA catalyst in dry SCR feed gas (purple), the total SO<sub>2</sub> uptake remains lower as compared to a preparation designed to maximize the formation of the  $[(\text{NH}_3)_4\text{Cu}_2^{\text{II}}\text{O}_2]^{2+}$  complex.

The measured SO<sub>2</sub> uptakes under different conditions are reflected in the NO<sub>x</sub> conversion measured at 200 °C in a dry SCR feed gas (Fig. 3). After exposure to SO<sub>2</sub> of the Cu-CHA

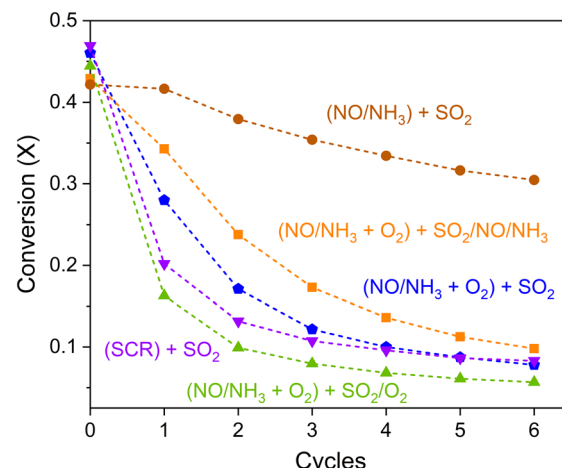
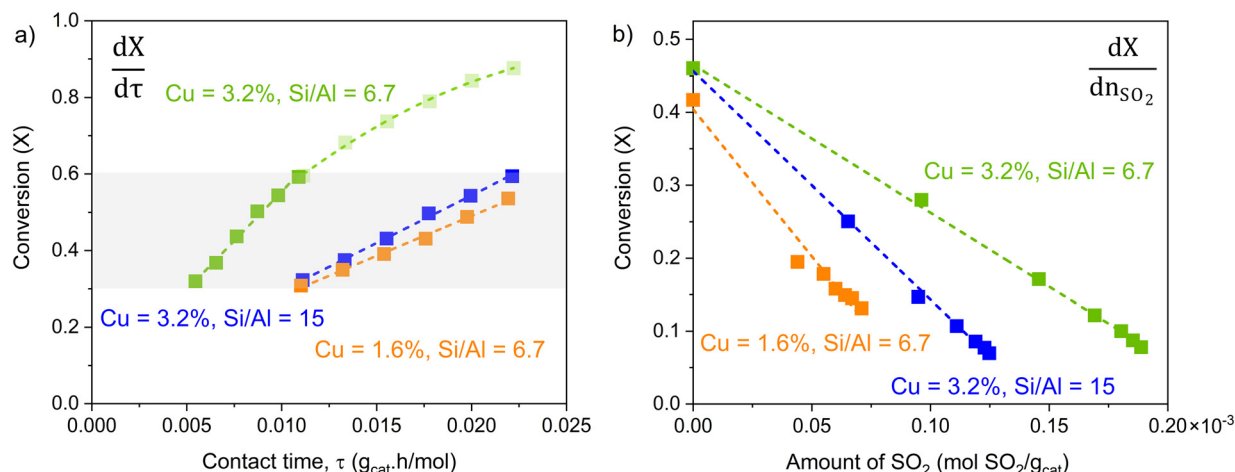


Fig. 3 NO conversion for Cu-CHA catalysts with Cu loading 3.2 wt% and Si/Al ratio of 6.7 at 200 °C, under the conditions of SO<sub>2</sub> exposure to reduced Cu<sup>I</sup> (brown), SO<sub>2</sub> exposure to the  $[(\text{NH}_3)_4\text{Cu}_2^{\text{II}}\text{O}_2]^{2+}$  complex (blue), SO<sub>2</sub> in presence of O<sub>2</sub> (green) or NO/NH<sub>3</sub> mixture (orange) to the  $[(\text{NH}_3)_4\text{Cu}_2^{\text{II}}\text{O}_2]^{2+}$  complex, and SO<sub>2</sub> exposure after exposure to dry SCR reaction gas mixture (purple). SO<sub>2</sub> concentration: 100 ppm.





**Fig. 4** a) Fractional conversion versus contact time and b) fractional conversion versus the total amount of SO<sub>2</sub> uptake at contact time of 0.0166 g<sub>cat</sub> h mol<sup>-1</sup> for catalyst with 1.6 wt% Cu and Si/Al ratio of 6.7 and catalyst with 3.2 wt% Cu and Si/Al ratio of 15 and contact time of 0.0076 g<sub>cat</sub> h mol<sup>-1</sup> for catalyst with 3.2 wt% Cu and Si/Al ratio of 6.7 based on the SO<sub>2</sub> exposure of the  $[(\text{NH}_3)_4\text{Cu}_2^{\text{II}}\text{O}_2]^{2+}$  complex. The grey-shaded area in the left panel indicates the data points used for the analysis.

catalyst to a Cu<sup>I</sup> state (brown), the NOx conversion shows a minor gradual decrease, indicating a limited impact of the SO<sub>2</sub> exposure on activity. Exposure of the catalyst to SO<sub>2</sub> after formation of the  $[(\text{NH}_3)_4\text{Cu}_2^{\text{II}}\text{O}_2]^{2+}$  complex has a much stronger impact on the NOx conversion (blue), reaching a stable level after 3 cycles, in line with the faster uptake of SO<sub>2</sub> under those conditions. Similarly, in the presence of a NO/NH<sub>3</sub> mixture, the exposure to SO<sub>2</sub> results in a more gradual decrease in NOx conversion (orange), and the conversion when the  $[(\text{NH}_3)_4\text{Cu}_2^{\text{II}}\text{O}_2]^{2+}$  complex is exposed to SO<sub>2</sub>/O<sub>2</sub> is the lowest (green). These results indicate that the uptake of SO<sub>2</sub> determines the activity of the catalyst, and therefore, the SO<sub>2</sub> uptake seems a suitable parameter to describe the deactivation of Cu-CHA catalysts for NH<sub>3</sub>-SCR.

Fig. 4 shows the experimental data after reduction, oxidation (the formation of  $[(\text{NH}_3)_4\text{Cu}_2^{\text{II}}\text{O}_2]^{2+}$  complex) and SO<sub>2</sub> exposure as described in sect. 2.2 to describe the deactivation behavior, according to the method described above (eqn 3). The left panel shows the measured conversions for different contact times  $\tau$ , corresponding to the rates, for the three catalysts used in this study. For the analysis of the deactivation in this particular data set, we use data points that show a conversion in the range 0.3–0.6, corresponding to the grey shaded area in Fig. 4. In this range, the measured conversions are adequately described by a linear dependence on the contact time, and the value for  $dX/d\tau$  is then found from the slope in this range (see Table 1). Because the slope of the lines reflects the reaction rates, it is clear that the 3.2 wt% Cu (Si/Al = 6.7) catalyst is more active than the other

two catalysts. This leads to the higher conversion for contact times between 0.011 and 0.022 g<sub>cat</sub> h mol<sup>-1</sup>, and the curve becomes more flat as the conversion approaches 1.

The right panel in Fig. 4 shows the change in conversion with increasing uptake of SO<sub>2</sub>, obtained in a series with 6 cycles of reduction, oxidation, and SO<sub>2</sub> exposure as described in sect. 2.2. The exposure to SO<sub>2</sub> was done using a mixture of 100 ppm SO<sub>2</sub> in N<sub>2</sub> for these measurements. For all three catalysts, the measured conversions can be approximated with a linear function, with a slope that corresponds to  $dX/dn_{\text{SO}_2}$ , listed in Table 1. Division of these values by the rates, as determined above, yields the SO<sub>2</sub>-sensitivity, which measures the deactivation by SO<sub>2</sub> (see Table 1). The results indicate that, with an SO<sub>2</sub>-sensitivity of  $-39$  g<sub>cat</sub> h mol<sup>-2</sup>, the 3.2 wt% Cu-CHA (Si/Al = 6.7) catalyst is less affected by the exposure to SO<sub>2</sub>, as compared to the other two catalysts, suggesting that a low Si/Al ratio of the chabazite, and higher Cu-content contribute to the SO<sub>2</sub> tolerance of Cu-CHA catalysts for NH<sub>3</sub>-SCR. The negative value of the SO<sub>2</sub> sensitivity reflects the decrease in effective contact time  $\tau$  or catalyst mass in the reactor as a consequence of the deactivation.

As mentioned, varying the conditions for the exposure to SO<sub>2</sub> leads to different SO<sub>2</sub> uptakes and different conversion levels after 6 cycles (see Fig. 2, 3 and Tables S1–S3†). The incremental increase in SO<sub>2</sub> uptake decreases in the consecutive SO<sub>2</sub>-exposure cycles, and the SO<sub>2</sub> uptake seems to approach a saturation level that depends on the conditions before or during the SO<sub>2</sub> exposure. We use these saturation levels as a starting

**Table 1** Determination of the SO<sub>2</sub> sensitivity from the experimental data (see Fig. 2) for the three catalysts

Si/Al ratio	Cu cont. (wt%)	Rate $dX/d\tau$ (mol g <sub>cat</sub> <sup>-1</sup> h <sup>-1</sup> )	$dn_{\text{SO}_2}/d\tau$ (g <sub>cat</sub> mol <sup>-1</sup> )	SO <sub>2</sub> sensitivity $dX/dn_{\text{SO}_2}$ (g <sub>cat</sub> <sup>2</sup> h mol <sup>-2</sup> )
6.7	1.6	20.1	-4033	-193
6.7	3.2	51.38	-2029	-39
15	3.2	24.9	-3134	-126



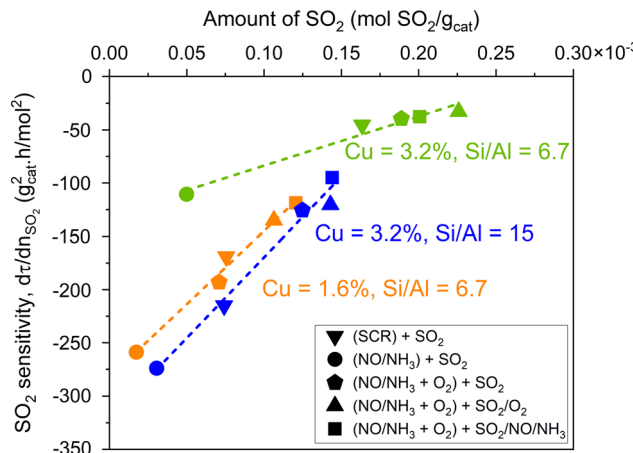


Fig. 5 SO<sub>2</sub> sensitivity as function of total SO<sub>2</sub> uptake after 6 cycles (see also Fig. 3).

point to determine how the deactivation depends on the SO<sub>2</sub> uptake, because the catalyst does not seem to change upon additional oxidation/SO<sub>2</sub> exposure cycles. Therefore, we do not expect the activity measurement itself to change the catalyst either. For each data set, a value for the SO<sub>2</sub>-sensitivity can be evaluated, using the method described above; an overview of the data is provided in the ESI† (Fig. S6–S9). Fig. 5 summarizes the values of for the SO<sub>2</sub>-sensitivity and SO<sub>2</sub> uptake for the three catalysts studied, under different conditions for SO<sub>2</sub> exposure. For all three catalysts, the SO<sub>2</sub> sensitivity is more negative at low SO<sub>2</sub> uptake, indicating that the impact of SO<sub>2</sub> is strongest at low SO<sub>2</sub> uptake, after which it decays linearly as the SO<sub>2</sub> content in the catalyst increases.

Table 2 summarizes the values for slope and intercept for a linear regression of the data points in Fig. 4, resulting in explicit expressions for the SO<sub>2</sub> sensitivity as a function of the total uptake of SO<sub>2</sub>. Using these values, we obtain a differential equation for the contact time  $\tau$ , and integration of these expressions result in a second order dependence on the SO<sub>2</sub> uptake. However, this integration step still requires a correct quantification of the values for  $\tau$ . We have used the measured conversion and SO<sub>2</sub> uptake after the cycles using a mixture of 100 ppm SO<sub>2</sub>/10%O<sub>2</sub> for the SO<sub>2</sub> exposure for that purpose, because it generally results in the strongest deactivation. In this way, the model covers the entire measured range of deactivation. Then, it is possible to calculate a value for  $\tau$  at different SO<sub>2</sub> uptake values, shown in Fig. 6. The shaded bands represent the ranges based on the estimated errors for the slope and intercept values in the linear regression. This dependence of the contact time  $\tau$  on the amount of SO<sub>2</sub> describes the deactivation behavior for the three catalysts.

Once the variation of the contact time  $\tau$  is known, the corresponding NO<sub>x</sub> conversions can be calculated using the rate from Fig. 4a for each catalyst. By considering the rate of the NH<sub>3</sub>-SCR reaction are derived from the activity measurements of the fresh catalysts, the NO<sub>x</sub> conversion ( $X_{NO_x}$ ) then becomes:

$$X_{NO_x} = \text{rate} \cdot \tau(n_{SO_2}) \quad (4)$$

where rate is evaluated for the fresh catalysts, and  $\tau$  is the effective contact time as shown in Fig. 6 at a given SO<sub>2</sub> amount  $n_{SO_2}$ .

Fig. 7 displays the calculated NO<sub>x</sub> conversion together with the measured values obtained after six SO<sub>2</sub> exposure cycles. The shaded areas represent the error margins for the calculated NO<sub>x</sub> conversion, taking into account the statistical error in the linear regression parameters, as listed in Table 2. These results indicate that the model results in a fair description of the observed deactivation, considering the variations of the conditions for SO<sub>2</sub> exposure. It seems that different impacts of SO<sub>2</sub> under different conditions is reflected in total uptake of SO<sub>2</sub> in the catalyst, making the total SO<sub>2</sub> uptake a suitable record of the catalyst history, as far as deactivation by SO<sub>2</sub> is concerned. Finally, we realize that the fair description of SO<sub>2</sub> deactivation is to a large degree due to the choice to normalize the data based on the measured conversion after SO<sub>2</sub> exposure cycles in the presence of 10% O<sub>2</sub>, leading to a high uptake of SO<sub>2</sub>.

## 4 Discussion

In the analysis above, the deactivation of Cu-CHA catalysts for NH<sub>3</sub>-SCR by SO<sub>2</sub> is a consequence of SO<sub>2</sub> uptake by the Cu-CHA catalyst, most probably *via* an interaction with the  $[(NH_3)_4Cu^{II}O_2]^{2+}$  complex.<sup>27,28,34</sup> Following the concept of a non-selective deactivation, the observed decrease in NO<sub>x</sub> conversion is expressed as an effective loss of active catalyst to quantify the deactivation. This leads to the SO<sub>2</sub> sensitivity ( $dt/dn_{SO_2}$ ) as the measure for the deactivation. Because the SO<sub>2</sub> sensitivity reflects a loss of active catalyst, its value is given as a negative number.

A result of this study is that the SO<sub>2</sub> sensitivity becomes less negative with increasing SO<sub>2</sub> uptake, indicating that impact of SO<sub>2</sub> on the catalyst activity is highest at low SO<sub>2</sub> contents in the catalyst, and becomes weaker as the SO<sub>2</sub> uptake increases. This result is well in line with the observation that most of the deactivation takes place at S/Cu ratios below 0.5,<sup>11,12,19,40</sup> before a stable activity of about 5–10% of the initial activity is reached. In fact, the highest uptake of SO<sub>2</sub> encountered in this study is about  $0.20\text{--}0.25 \times 10^{-3}$  mol g<sub>cat</sub><sup>-1</sup> for the 3.2 wt% Cu (Si/Al = 6.7)

Table 2 Linear regression parameters for the data in Fig. 5, describing the dependence of the SO<sub>2</sub> sensitivity as a function of SO<sub>2</sub> uptake

Si/Al ratio	Cu cont. (wt%)	Slope	Intercept	R <sup>2</sup>
6.7	1.6	$1.375 \pm 0.0926$	$-0.283 \pm 0.0079$	0.986
6.7	3.2	$0.464 \pm 0.0528$	$-0.130 \pm 0.0093$	0.962
15	3.2	$1.51 \pm 0.1145$	$-0.322 \pm 0.0128$	0.983



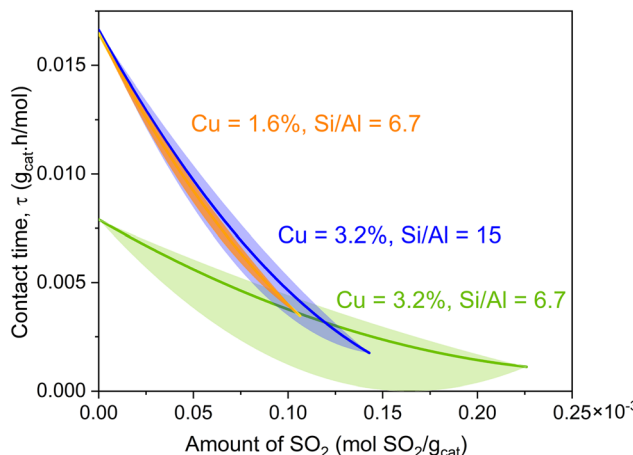


**Fig. 6** Calculated variations of contact time with  $\text{SO}_2$  uptake, based on the regression relations given in Table 2. The bands represent the margins based on the estimated errors in the regression parameters.

catalyst, corresponding to a molar S/Cu ratio of 0.4–0.5, indicating that the uptake of  $\text{SO}_2$  in general is limited. Nevertheless, the measured  $\text{NO}_x$  conversion for this catalyst decreases from 0.4 to well below 0.1 (see Fig. 7). Our results show that the deactivation is most pronounced at low uptakes of  $\text{SO}_2$  and that the final residual activity is not affected by further  $\text{SO}_2$  exposure, even though the uptake is still well below a S/Cu ratio of 1. To the best of our knowledge, most of the reports in the literature agree with the observation that the deactivation by  $\text{SO}_2$  could be severe, but typically not complete.<sup>10,18,41–43</sup>

These observations are difficult to align with a deposition of ammonium sulfate leading to pore blocking, which is often cited as the reason for the catalyst deactivation by  $\text{SO}_2$ .<sup>16–18,44</sup> First, recent DFT calculations show that a single ammonium sulfate unit in a cage does not reduce SCR activity; however, at least two sulfate units leads to a reduction.<sup>44</sup> Second, if ammonium sulfate is formed as long as the  $\text{NH}_3$ -SCR reaction occurs, then the catalyst is expected to eventually deactivate

completely, and not leave a residual activity.<sup>10,11,18,42</sup> Both these arguments support the conclusion that small amounts of  $\text{SO}_2$  have a minimal impact on SCR activity. Full catalyst deactivation through pore blocking requires a critical amount of S (as ammonium sulfate) to block the pores and limit access to the Cu ions at 200 °C. Therefore, it seems more likely that the deactivation by  $\text{SO}_2$  involves a direct impact of  $\text{SO}_2$  on the reactivity of the active Cu in the catalyst, which has been further confirmed by X-ray and UV-vis spectroscopy.<sup>27–29,34</sup>

The strong impact of  $\text{SO}_2$  at low amounts of  $\text{SO}_2$  seems to harmonize with a reaction mechanism proposed earlier.<sup>28</sup> The reaction of  $\text{SO}_2$  with the  $[(\text{NH}_3)_4\text{Cu}_2^{\text{II}}\text{O}_2]^{2+}$  complex results in the reduction of the  $\text{Cu}^{\text{II}}$  to  $\text{Cu}^{\text{I}}$  and the formation of a mobile sulfate-like intermediate. In a subsequent step, this sulfate-like intermediate reacts with a second  $[(\text{NH}_3)_4\text{Cu}_2^{\text{II}}\text{O}_2]^{2+}$  complex.<sup>28</sup> According to that mechanism, a single  $\text{SO}_2$  molecule effectively dissociates two  $[(\text{NH}_3)_4\text{Cu}_2^{\text{II}}\text{O}_2]^{2+}$  complexes, thus affecting four Cu ions, which supports the result that a small amount of  $\text{SO}_2$  already leads to severe deactivation. As the  $\text{SO}_2$  uptake increases, less  $[(\text{NH}_3)_4\text{Cu}_2^{\text{II}}\text{O}_2]^{2+}$  complexes are available, and the impact of  $\text{SO}_2$  diminishes as the  $\text{SO}_2$  uptake increases, in line with our observation of a weaker impact of  $\text{SO}_2$  with increasing  $\text{SO}_2$  uptake. Note that this interpretation applies primarily to deactivation at 200 °C. At higher temperatures, there are two counteracting effects, namely an increased reactivity of  $\text{SO}_2$  due to the higher temperature, but also a possible decomposition of  $[(\text{NH}_3)_4\text{Cu}_2^{\text{II}}\text{O}_2]^{2+}$  complexes, which reduces their availability leading to a lower  $\text{SO}_2$  uptake. However, the precise thermal stability of the  $[(\text{NH}_3)_4\text{Cu}_2^{\text{II}}\text{O}_2]^{2+}$  complex is not known at present. We also note that exposure to  $\text{SO}_2$  results in a lower reactivity of the Cu towards NO, which is reflected in an increase in reaction temperature from about 120 °C to 300 °C, but not to a complete deactivation.<sup>35</sup> Treatments at this temperature (300 °C) are typically not sufficient to regenerate the catalyst after poisoning by  $\text{SO}_x$ , as reported by many authors.<sup>9,10,36,42,43,45,46</sup> Following this reasoning, the residual  $\text{NH}_3$ -SCR activity observed after high exposure to  $\text{SO}_2$  is possibly a reflection of this slower reaction of NO with the Cu after exposure to  $\text{SO}_2$ .

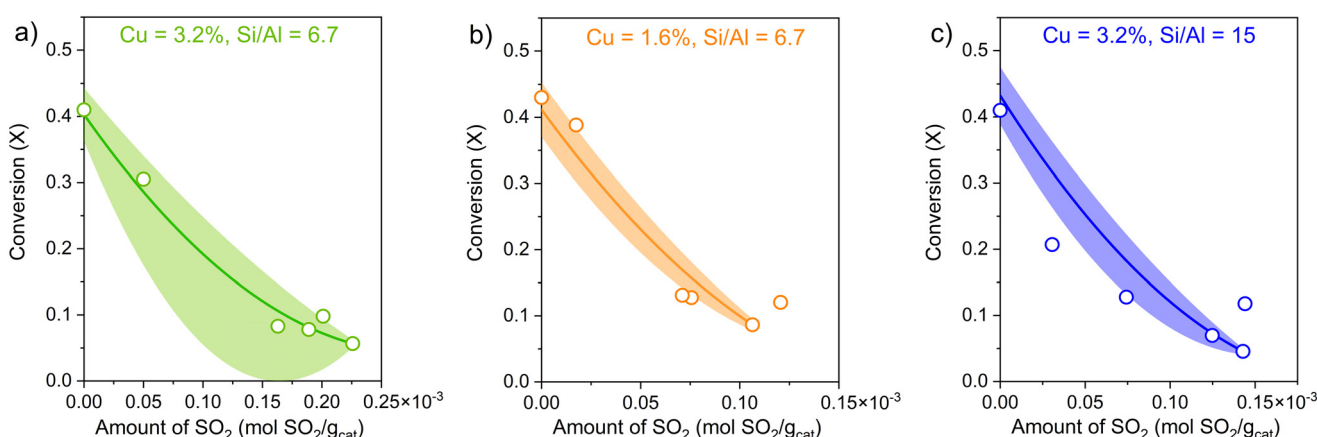


**Fig. 7** Calculated (solid lines) and measured (circle points)  $\text{NO}_x$  conversions at 200 °C after six  $\text{SO}_2$  exposure cycles for Cu-CHA catalysts with a) 3.2 wt% Cu and Si/Al = 6.7, b) 0.8 wt% Cu and Si/Al = 6.7 and c) 3.2 wt% Cu and Si/Al = 15. The shaded areas represent the error based on the regression constants given in Table 2.



Bjerregaard *et al.* have proposed a different mechanism for the deactivation by  $\text{SO}_2$ , based on a reaction model for the  $\text{NH}_3\text{-SCR}$  reaction in the presence of  $\text{SO}_2$  derived from density functional theory (DFT) calculations.<sup>44</sup> In their mechanism,  $\text{SO}_2$  reacts with the  $[(\text{NH}_3)_4\text{Cu}^{\text{II}}\text{O}_2]^{2+}$  complex as well, but dissociation of the complex and reduction to  $\text{Cu}^{\text{I}}$  takes first place after reaction with an  $\text{NO}$  molecule. The modified cycle for SCR then leads to accumulation of sulfate compounds in the catalysts, which limits the accessibility of the Cu-sites in the catalyst. This model disagrees on two points from the interpretation derived above: (1) experiments have shown that the reduction of  $\text{Cu}^{\text{II}}$  in the  $[(\text{NH}_3)_4\text{Cu}^{\text{II}}\text{O}_2]^{2+}$  complex by  $\text{SO}_2$  also takes place in the absence of  $\text{NO}$ .<sup>27–29</sup> (2) the conclusion that deactivation is caused by limiting access to the Cu sites as sulfate compounds accumulate in the catalyst implies that the Cu-CHA catalysts have a measurable tolerance for  $\text{SO}_2$ , in contrast to the results presented here.

The data presented in Fig. 4 show that the catalyst with the highest Cu content (3.2 wt%) and lowest Si/Al ratio (6.7) is less sensitive to  $\text{SO}_2$ , and therefore these catalysts show a better resistance to  $\text{SO}_2$ , as compared to the other two catalysts. An indication for a possible reason behind this trend is obtained from *in situ* X-ray absorption spectroscopy. Cu-CHA catalysts with a low Si/Al ratio show a lower fraction of  $\text{Cu}^{\text{I}}$  under reaction conditions for  $\text{NH}_3\text{-SCR}$ , which indicates a difference in reducibility of the  $[(\text{NH}_3)_4\text{Cu}^{\text{II}}\text{O}_2]^{2+}$  complex. This seems to be related to the presence of a bent configuration of the  $[(\text{NH}_3)_4\text{Cu}^{\text{II}}\text{O}_2]^{2+}$  complex in catalysts with a high Si/Al ratio.,<sup>34,47</sup> which may affect the interaction of Cu-CHA with  $\text{SO}_2$  in a similar way.

A semi-quantitative UV-vis analysis shows larger changes in UV spectra following  $\text{SO}_2$  uptake in the catalyst with a low Si/Al ratio (6.7), in line with the higher uptake of  $\text{SO}_2$  for the 3.2 wt% Cu-CHA (Si/Al = 6.7) shown in Fig. 2, suggesting a correlation with the formation of the  $[(\text{NH}_3)_4\text{Cu}^{\text{II}}\text{O}_2]^{2+}$  complex.<sup>29</sup> However, the estimated change in absorption coefficient, based on the stoichiometry of the reaction of  $[(\text{NH}_3)_4\text{Cu}^{\text{II}}\text{O}_2]^{2+}$  with  $\text{SO}_2$ , does not seem to change with the Si/Al ratio, indicating that the  $\text{SO}_2$  is bound in a similar way in all catalysts. In addition, the activity of the catalysts in the UV-vis study decreases by about 50% all catalysts, independent of the Si/Al ratio, in the first  $\text{SO}_2$  exposure cycle, followed by a further 50% decrease in the second  $\text{SO}_2$  exposure cycle, resulting in an overall activity loss of approximately 75%.<sup>29</sup> Because the  $\text{SO}_2$  uptake is higher for the 3.2 wt% Cu-CHA (Si/Al = 6.7) catalyst, while the impact on the deactivation is the same, this results in a lower  $\text{SO}_2$  sensitivity, as defined here in our study. This agrees well with the conclusion that the  $\text{SO}_2$  uptake is related to the ability of the catalyst to form the  $[(\text{NH}_3)_4\text{Cu}^{\text{II}}\text{O}_2]^{2+}$  complex.<sup>27,28,34</sup>

Another approach to the different impact of  $\text{SO}_2$  on Cu-CHA catalysts with low and high Si/Al ratio is a difference in reactivity of  $\text{Z}_2\text{-Cu}^{\text{II}}$ , which are abundant at low Si/Al ratio, and  $\text{Z}\text{-CuOH}$  groups, which are more abundant at high Si/Al ratios.<sup>42</sup> Because the reaction of  $\text{SO}_2$  with the Cu-CHA catalyst requires a  $[(\text{NH}_3)_4\text{Cu}^{\text{II}}\text{O}_2]^{2+}$  complex, the difference in reactivity of  $\text{SO}_2$  for  $\text{Z}\text{-CuOH}$  and  $\text{Z}_2\text{-Cu}^{\text{II}}$  is probably a reflection of a different ability

of  $\text{Z}\text{-CuOH}$  and  $\text{Z}_2\text{-Cu}^{\text{II}}$  to form Cu-pairs and  $[(\text{NH}_3)_4\text{Cu}^{\text{II}}\text{O}_2]^{2+}$  complexes.<sup>28,29,34</sup>

To construct a model for the performance of Cu-CHA catalysts upon  $\text{SO}_2$  exposure, a quantitative measurement of the deactivation behavior is needed. According to the procedure derived above, a minimum of 3 data points are needed, to characterize the deactivation, preferably the activity of the fresh catalyst, and a conversion after several  $\text{SO}_2$  exposure cycles with low  $\text{SO}_2$  uptake (high  $\text{Cu}^{\text{I}}$  content, reducing conditions) and high  $\text{SO}_2$  uptake (high content of  $[(\text{NH}_3)_4\text{Cu}^{\text{II}}\text{O}_2]^{2+}$  complex). However, even though the approach presented in this study seems to produce reasonable qualitative results, it is doubtful if a sufficiently accurate measurement can be obtained, since the results depend on the determination of the slopes  $dX/dn_{\text{SO}_2}$  and  $dX/d\tau$ , which can easily lead to larger errors. Furthermore, the presence of water during the exposure to  $\text{SO}_2$  can change the way of  $\text{SO}_2$  uptake, as formation of non-Cu bound sulfur, such as  $\text{H}_2\text{SO}_4$  could be formed.<sup>44</sup> The rather consistent results we have obtained in this study is probably due to the fact that under the conditions used in the measurements, the sulfur eventually is bound to the Cu ions in the catalyst.<sup>28,35</sup> Therefore, due to the sensitivity of the reaction of  $\text{SO}_2$  with the Cu-CHA catalyst to the reaction conditions, and the complexity of the chemistry behind that reaction, the approach to describe the deactivation of Cu-CHA catalysts by  $\text{SO}_2$  as a loss of catalyst amount, which has been successfully applied for methanol-to-hydrocarbon reactions,<sup>38,39</sup> does not seem very suitable to predict the behavior of a Cu-CHA catalyst in the dynamic environment of an exhaust system.

## 5 Conclusion

In this study, a descriptive model is developed for the deactivation of Cu-CHA catalysts for  $\text{NH}_3\text{-SCR}$  by  $\text{SO}_2$ , by expressing a loss in activity caused by  $\text{SO}_2$  exposure as a loss of catalyst amount. In order to avoid ambiguities in the quantification of the deactivation, the amount of  $\text{SO}_2$  accumulated in the catalyst is used as the descriptor for the deactivation process. The deactivation is then described in terms of  $d\tau/dn_{\text{SO}_2}$ , which can be interpreted as a sensitivity of the catalyst for  $\text{SO}_2$ . This sensitivity can be determined from the experimental data from the measured NOx conversions at different contact times, by variation of the flow, and at different amounts of  $\text{SO}_2$ , which is achieved by repeated oxidation and  $\text{SO}_2$  exposure steps.

The model was applied to three different Cu-CHA catalysts, namely 3.2 wt% Cu with Si/Al = 6.7, 3.2 wt% Cu with Si/Al = 15, and 1.6 wt% Cu with Si/Al = 6.7. The impact of  $\text{SO}_2$  on the activity, as indicated by the sensitivity, is strongest at low  $\text{SO}_2$  uptakes, after which the sensitivity declines linearly with increasing  $\text{SO}_2$  uptake. Furthermore, the catalyst with high Cu content and low Si/Al ratio shows a lower  $\text{SO}_2$  sensitivity, indicating a better tolerance for  $\text{SO}_2$  of such catalysts. A small amount of  $\text{SO}_2$ , corresponding to a molar  $\text{SO}_2/\text{Cu}$  ratio below 0.5, causes a strong decrease in the NOx conversion from about 0.4 to below 0.1, deactivation,



indicating that the deactivation is caused by a direct reaction of the SO<sub>2</sub> with the active Cu.

Because the SO<sub>2</sub> uptake is affected by the chemical conditions during SO<sub>2</sub> exposure, an accurate quantification of the SO<sub>2</sub> sensitivity from the experimental data in controlled oxidation/SO<sub>2</sub> exposure cycles is difficult, as it requires very accurate data for both activity and SO<sub>2</sub> uptake, in order to reliably determine a value for the differential  $dt/dn_{SO_2}$ . Furthermore, in the dynamic environment of exhaust systems, the chemical conditions change unpredictably, and therefore, the SO<sub>2</sub> uptake is unpredictable as well. Though a description of the deactivation in terms of SO<sub>2</sub> sensitivity can differentiate between catalyst materials with higher or lower sensitivity for SO<sub>2</sub>, the approach does not seem to produce a reliable quantification of the deactivation behavior to model the performance of Cu-CHA catalysts in exhaust systems upon exposure to SO<sub>2</sub>.

## Data availability

The data supporting this article have been included as part of the ESI.†

## Author contributions

RKA: experiments, data processing, writing – original draft. GB: funding, supervision, editing. TWJ: funding, conceptualization, data processing, writing – editing.

## Conflicts of interest

The authors declare no conflict of interest.

## Acknowledgements

We acknowledge support from the European Union's Horizon 2020 Research and Innovation Programme under the Marie Skłodowska-Curie grant agreement No. 955839 (CHASS) and from the Project CH4.0 under the MUR program "Dipartimenti di Eccellenza 2023-2027" (CUP: D13C22003520001).

## Notes and references

- 1 J. H. Kwak, R. G. Tonkyn, D. H. Kim, J. Szanyi and C. H. F. Peden, *J. Catal.*, 2010, **275**, 187–190.
- 2 I. Bull, W.-M. Xue, P. Burk, R. S. Boorse, W. M. Jaglowski, G. S. Koermer, A. Moini, J. A. Patchett, J. C. Dettling and M. T. Caudle, *US Pat.*, 2009, 7601662.
- 3 U. Deka, A. Juhin, E. A. Eilertsen, H. Emerich, M. A. Green, S. T. Korhonen, B. M. Weckhuysen and A. M. Beale, *J. Phys. Chem. C*, 2012, **116**, 4809–4818.
- 4 A. M. Beale, F. Gao, I. Lezcano-Gonzalez, C. H. Peden and J. Szanyi, *Chem. Soc. Rev.*, 2015, **44**, 7371–7405.
- 5 I. Lezcano-Gonzalez, U. Deka, B. Arstad, A. V. Y.-D. Deyne, K. Hemelsoet, M. Waroquier, V. V. Speybroeck, B. M. Weckhuysen and A. M. Beale, *Phys. Chem. Chem. Phys.*, 2014, **16**, 1639–1650.
- 6 D. W. Fickel and R. F. Lobo, *J. Phys. Chem. C*, 2010, **114**, 1633–1640.
- 7 M. Moliner, C. Franch, E. Palomares, M. Grill and A. Corma, *Chem. Commun.*, 2012, **48**, 8264.
- 8 F. Gao, E. D. Walter, M. Kollar, Y. Wang, J. Szanyi and C. H. F. Peden, *J. Catal.*, 2014, **319**, 1–14.
- 9 Y. Cheng, C. Lambert, D. H. Kim, J. H. Kwak, S. J. Cho and C. H. Peden, *Catal. Today*, 2010, **151**, 266–270.
- 10 K. Wijayanti, K. Xie, A. Kumar, K. Kamasamudram and L. Olsson, *Appl. Catal., B*, 2017, **219**, 142–154.
- 11 P. S. Hammershøi, A. D. Jensen and T. V. W. Janssens, *Appl. Catal., B*, 2018, **238**, 104–110.
- 12 P. S. Hammershøi, Y. Jangjou, W. S. Epling, A. D. Jensen and T. V. W. Janssens, *Appl. Catal., B*, 2018, **226**, 38–45.
- 13 X. Auvray, M. Arvanitidou, Å. Högström, J. Jansson, S. Fouladvand and L. Olsson, *Emiss. Control Sci. Technol.*, 2021, **7**, 232–246.
- 14 D. W. Brookshear, J. G. Nam, K. Nguyen, T. J. Toops and A. Binder, *Catal. Today*, 2015, **258**, 359–366.
- 15 L. Olsson, K. Wijayanti, K. Leistner, A. Kumar, S. Y. Joshi, K. Kamasamudram, N. W. Currier and A. Yezerets, *Appl. Catal., B*, 2016, **183**, 394–406.
- 16 L. Zhang, D. Wang, Y. Liu, K. Kamasamudram, J. Li and W. Epling, *Appl. Catal., B*, 2014, **156–157**, 371–377.
- 17 Y. Jangjou, D. Wang, A. Kumar, J. Li and W. S. Epling, *ACS Catal.*, 2016, **6**, 6612–6622.
- 18 K. Wijayanti, K. Leistner, S. Chand, A. Kumar, K. Kamasamudram, N. W. Currier, A. Yezerets and L. Olsson, *Catal. Sci. Technol.*, 2016, **6**, 2565–2579.
- 19 A. J. Shih, I. Khurana, H. Li, J. González, A. Kumar, C. Paolucci, T. M. Lardinois, C. B. Jones, J. D. Albarracín Caballero, K. Kamasamudram, A. Yezerets, W. N. Delgass, J. T. Miller, A. L. Villa, W. F. Schneider, R. Gounder and F. H. Ribeiro, *Appl. Catal., A*, 2019, **574**, 122–131.
- 20 J. Du, X. Shi, Y. Shan, G. Xu, Y. Sun, Y. Wang, Y. Yu, W. Shan and H. He, *Catal. Sci. Technol.*, 2020, **10**, 1256–1263.
- 21 S. Dahlin, C. Lantto, J. Englund, B. Westerberg, F. Regali, M. Skoglundh and L. J. Pettersson, *Catal. Today*, 2019, **320**, 72–83.
- 22 B. B. Hansen, P. S. Hammershøi, F. H. Fagerberg, S. I. Hansen, X. B. Sjögren, P. N. R. Vennestrøm, A. D. Jensen and T. V. W. Janssens, *Emiss. Control Sci. Technol.*, 2024, **10**, 204–212.
- 23 M. Iwasaki, *Urea-SCR Technology for DeNOx After Treatment of Diesel Exhausts*, Springer, New York, NY, 2014, pp. 221–246.
- 24 Y. M. Liu, H. Shu, Q. S. Xu, Y. H. Zhang and L. J. Yang, *J. Fuel Chem. Technol.*, 2015, **43**, 1018–1024.
- 25 Y. Qiu, C. Fan, C. Sun, H. Zhu, W. Yi, J. Chen, L. Guo, X. Niu, J. Chen, Y. Peng, T. Zhang and J. Li, *Catalysts*, 2020, **10**, 1–12.
- 26 Y. Wang, Z. Li, R. Fan, X. Guo, C. Zhang, Y. Wang, Z. Ding, R. Wang and W. Liu, *Catalysts*, 2019, **9**, 797.
- 27 A. Y. Molokova, E. Borfecchia, A. Martini, I. A. Pankin, C. Atzori, O. Mathon, S. Bordiga, F. Wen, P. N. R. Vennestrøm, G. Berlier, T. V. W. Janssens and K. A. Lomachenko, *JACS Au*, 2022, **2**, 787–792.



- 28 A. Y. Molokova, R. K. Abasabadi, E. Borfecchia, O. Mathon, S. Bordiga, F. Wen, G. Berlier, T. V. W. Janssens and K. A. Lomachenko, *Chem. Sci.*, 2023, **14**, 11521–11531.
- 29 R. K. Abasabadi, T. V. W. Janssens, S. Bordiga and G. Berlier, *Catal. Sci. Technol.*, 2024, **14**, 3076–3085.
- 30 C. Paolucci, I. Khurana, A. A. Parekh, S. Li, A. J. Shih, H. Li, J. R. Di Iorio, J. D. Albarracin-Caballero, A. Yezerets, J. T. Miller, W. N. Delgass, F. H. Ribeiro, W. F. Schneider and R. Gounder, *Science*, 2017, **357**, 898–903.
- 31 L. Chen, T. V. W. Janssens and H. Grönbeck, *Phys. Chem. Chem. Phys.*, 2019, **21**, 10923–10930.
- 32 L. Chen, T. V. W. Janssens, P. N. R. Vennestrøm, J. Jansson, M. Skoglundh and H. Grönbeck, *ACS Catal.*, 2020, **10**, 5646–5656.
- 33 C. Negri, T. Selleri, E. Borfecchia, A. Martini, K. A. Lomachenko, T. V. W. Janssens, M. Cutini, S. Bordiga and G. Berlier, *J. Am. Chem. Soc.*, 2020, **142**, 15884–15896.
- 34 T. V. W. Janssens, E. Borfecchia, K. A. Lomachenko, H. Grönbeck and G. Berlier, *ChemCatChem*, 2024, **16**, 1–20.
- 35 A. Y. Molokova, D. Salusso, E. Borfecchia, F. Wen, S. Magliocco, S. Bordiga, T. V. W. Janssens, K. A. Lomachenko and G. Berlier, *Catal. Sci. Technol.*, 2024, **14**, 5989–5995.
- 36 A. Kumar, M. A. Smith, K. Kamasamudram, N. W. Currier, H. An and A. Yezerets, *Catal. Today*, 2014, **231**, 75–82.
- 37 D. Yao, J. Hu, Y. Zhang, X. Hu, H. He, W. Jin, J. Wu and F. Wu, *Catal. Sci. Technol.*, 2025, **15**, 1547–1556.
- 38 B. L. Foley, B. A. Johnson and A. Bhan, *ACS Catal.*, 2019, **9**, 7065–7072.
- 39 T. V. W. Janssens, *J. Catal.*, 2009, **264**, 130–137.
- 40 P. S. Hammershøi, A. L. Godiksen, S. Mossin, P. N. R. Vennestrøm, A. D. Jensen and T. V. W. Janssens, *React. Chem. Eng.*, 2019, **4**, 1081–1089.
- 41 A. Kumar, M. A. Smith, K. Kamasamudram, N. W. Currier and A. Yezerets, *Catal. Today*, 2016, **267**, 10–16.
- 42 Y. Jangjou, Q. Do, Y. Gu, L. G. Lim, H. Sun, D. Wang, A. Kumar, J. Li, L. C. Grabow and W. S. Epling, *ACS Catal.*, 2018, **8**, 1325–1337.
- 43 V. Mesilov, S. Dahlin, S. L. Bergman, S. Xi, J. Han, L. Olsson, L. J. Pettersson and S. L. Bernasek, *Appl. Catal., B*, 2021, **299**, year.
- 44 J. D. Bjerregaard, M. Votsmeier and H. Grönbeck, *J. Catal.*, 2023, **417**, 497–506.
- 45 S. Dahlin, C. Lantto, J. Englund, B. Westerberg, F. Regali, M. Skoglundh and L. J. Pettersson, *Catal. Today*, 2019, **320**, 72–83.
- 46 J. Luo, D. Wang, A. Kumar, J. Li, K. Kamasamudram, N. Currier and A. Yezerets, *Catal. Today*, 2016, **267**, 3–9.
- 47 A. Martini, C. Negri, L. Bugarin, G. Deplano, R. K. Abasabadi, K. A. Lomachenko, T. V. W. Janssens, S. Bordiga, G. Berlier and E. Borfecchia, *J. Phys. Chem. Lett.*, 2022, **13**, 6164–6170.

